

Vector and parameters for targeted transgenic RNA interference in *Drosophila melanogaster*

Jian-Quan Ni^{1,2,5}, Michele Markstein^{1,5},
Richard Binari^{1,2,5}, Barret Pfeiffer³, Lu-Ping Liu^{1,2},
Christians Villalta^{1,2}, Matthew Booker¹,
Lizabeth Perkins⁴ & Norbert Perrimon^{1,2}

The conditional expression of hairpin constructs in *Drosophila melanogaster* has emerged in recent years as a method of choice in functional genomic studies. To date, upstream activating site-driven RNA interference constructs have been inserted into the genome randomly using P-element-mediated transformation, which can result in false negatives due to variable expression. To avoid this problem, we have developed a transgenic RNA interference vector based on the phiC31 site-specific integration method.

Transgenic RNA interference (RNAi) has emerged as an important method for analyzing gene function in *D. melanogaster* and has joined the already rich arsenal of tools available for functional genomic studies in this organism¹. The method relies on the Gal4–upstream activating site (UAS) system² to control the expression of a gene fragment that is dimerized to produce a double-stranded RNA (dsRNA) hairpin structure, which then triggers a sequence-specific post-transcriptional silencing and RNAi response. Tissue- or cell-specific expression of the transgenic RNAi constructs is achieved after a cross between UAS-hairpin and Gal4 driver lines. The main advantage of the method, in addition to its relatively simple design and fast execution time, is that it allows spatial and temporal control of the knockdown construct, which is essential for characterizing genes with pleiotropic functions.

A problem with current methodology is the variability in the level of hairpin expression due to the random integration in the genome of the P-element-based UAS-hairpin constructs. For example, one recent report in which two random insertions per construct were tested showed that in 40% of cases the two behaved differently, with one insertion showing lethality and the other viability when tested with the ubiquitously expressed actin5C-Gal4 driver¹. To avoid the high incidence of false negatives

resulting from random integration, we decided to develop a vector for transgenic RNAi based on the phiC31 targeted integration method³. Targeting RNAi hairpin constructs to a specific region of the genome with the phiC31 integrase method offers a number of advantages over P-element-based methods, in regard to both speed of production and potency of the transgenic RNAi lines. Thus, we expect the penetrance (percentage of lines that show noteworthy phenotypes) to be higher when UAS-driven hairpins are targeted to specific attP sites that allow for consistently robust expression levels. (Our decision to use the attP2 docking site was based on observations of M.M. and N.P. (unpublished data) demonstrating optimal basal and inducible properties.) Moreover, by targeting hairpins to the same sites, we can make side-by-side comparisons between different hairpins directed against the same gene, allowing for reliable validation of the RNAi hairpin phenotypes with multiple constructs.

We built Valium (Vermilion-AttB-Loxp-Intron-UAS-MCS) (Fig. 1a), a transgenic RNAi vector based on the phiC31 site-specific integration method, and generated hairpins directed against a number of genes with known phenotypes (Supplementary Table 1 online and data not shown). To avoid potential off-target effects, which have been shown to be a significant source of false positives in cell-based *D. melanogaster* RNAi screens⁴, we designed the hairpin sequences so that they do not contain short homology stretches of ≥ 19 nucleotides (Supplementary Methods online). Further, to evaluate the differences in potency between different hairpins directed against the same genes, we generated two hairpins per gene when possible.

We chose a set of 11 genes encoding proteins well known for their functions in wing development and crossed them to the *engrailed-Gal4* (*en-Gal4*) driver to allow us to detect phenotypes in the posterior wing compartment. The phenotypes generated were specific and expected (Fig. 1 and Supplementary Table 1). Knockdown of the epidermal growth factor receptor (*EGFR*) gene led to defects in growth and vein formation (Fig. 1b). A similar phenotype was observed with RNAi lines against *son of sevenless* (*sos*), which encodes a downstream transducer of the EGFR. RNAi directed against the *sprouty* (*sty*) gene was consistent with the protein's wild-type role as a negative regulator of EGFR in wing vein patterning. Knockdown of *decapentaplegic* (*dpp*) removed all veins, as expected (data not shown). Notably, knockdowns of the genes *dome*, *hop* and *STAT92E*, which encode three components of the JAK/STAT pathway (the receptor *domeless*, the JAK kinase *hopscotch* and the transcription factor *STAT92E*, respectively), all produced the same ectopic vein phenotype previously reported for classical mutants of these genes (Fig. 1c). The vein phenotype associated with knockdown of *cubitus interruptus* (*ci*) (Fig. 1e)

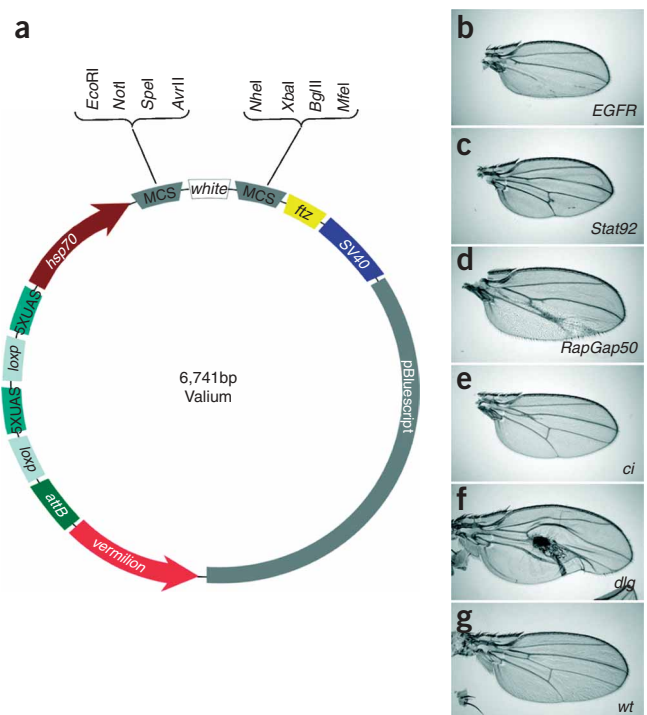
¹Department of Genetics and ²Howard Hughes Medical Institute, Harvard Medical School, 77 Avenue Louis Pasteur, Boston, Massachusetts 02175, USA. ³Howard Hughes Medical Institute, Janelia Farm Research Campus, 19700 Helix Drive, Ashburn, Virginia 20147, USA. ⁴Pediatric Surgical Research Labs, Massachusetts General Hospital, Harvard Medical School, 185 Cambridge Street, CPZN6.222, Boston, Massachusetts 02114, USA. ⁵These authors contributed equally to this work. Correspondence should be addressed to N.P. (perrimon@receptor.med.harvard.edu).

Figure 1 | Valium is an effective vector for transgenic RNAi. **(a)** Structure of Valium: Valium contains *vermillion* as the selectable marker⁹; an attB sequence to allow for phiC31 targeted integration at genomic attP landing sites³; two pentamers of UAS, one of which can be removed using the Cre-loxP system¹⁰; the hsp70 TATA promoter; a multiple cloning site (MCS) that allows a single PCR product to be cloned in both orientations to generate the hairpin construct; the *white* intron, located between the two halves of the inverted DNA repeat, which has been shown to reduce toxicity in bacteria; and the *ftz* intron, followed by the SV40 poly(A) tail, to facilitate hairpin RNA expression, processing and export from the nucleus. We chose *vermillion* rather than *mini-white* because the exact gene dosage of *white* has been found to be important in behavioral studies¹¹. **(b–g)** Examples of hairpin-induced wing phenotypes in *en-Gal4*; *UAS-hairpin* flies. Note that the various phenotypes generated have no common features, indicating that there are no nonspecific patterning defects generated as a result of general overexpression of dsRNAs. Further, control hairpins do not show any unusual wing phenotypes (data not shown).

as well as the polarity defects caused by knockdown of *armadillo* (*arm*) were consistent with the reported functions of these proteins in vein and wing margin formation, respectively. Knockdown of *discs-large* (*dlg1*) caused a crumpled and necrotic wing phenotype that is most likely due to a loss of apical-basal polarity and overproliferation (Fig. 1f). Finally, knockdown of *RacGap50C* (also known as *tum*) generated a range of defects, including increased width and fusion of veins and enlarged cells (Fig. 1d). A description of the wing-mutant phenotypes of the genes tested here can be found at FlyBase. Notably, in the seven cases in which two independent hairpin lines were generated (Supplementary Table 1), their phenotypes were very similar if not identical, suggesting that the specific phenotypes obtained with these hairpins are due to knockdown of the intended gene and not to off-target effects. Further, expression of hairpin constructs directed against control dsRNAs did not generate patterning defects¹ (data not shown).

Notably, we consistently observed a stronger effect in males than in females, most likely reflecting a difference in the level of hairpin expression. The origin of this effect is unclear and could be due to a difference in developmental timing between males and females. Hairpin constructs may produce a higher abundance of dsRNAs in males because they develop slightly more slowly than females. Alternatively, this phenomenon may be due to dosage compensation, as the transgenes contain X-linked sequences of the *white* intron and the *vermillion* gene as well as being inserted in an attP site flanked by the *yellow* gene that originates from the X chromosome.

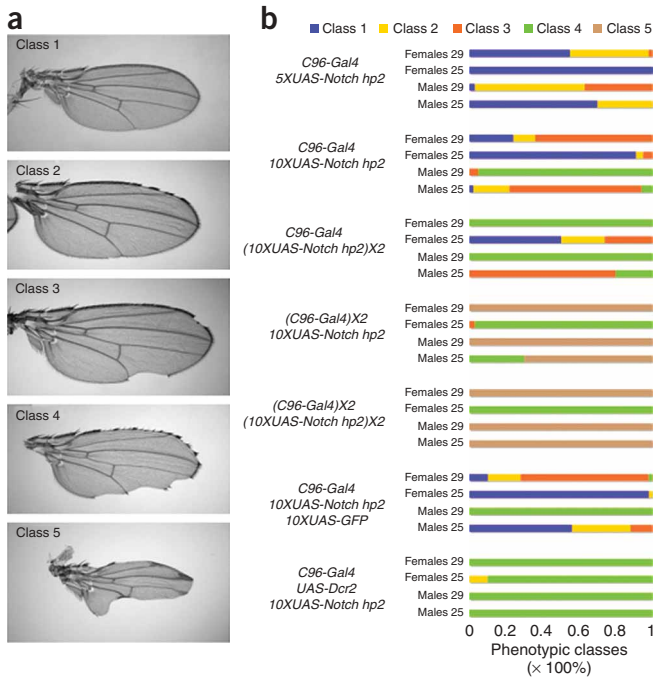
Compared to P-element-based transgenic RNAi, the targeted insertion RNAi method has several practical advantages. The frequency at which transformants are recovered using the integrase method is almost fivefold higher than that obtained using conventional P-element transformation^{3,5} (unpublished observations). No mapping of the transformants to a specific chromosome is needed, and insertions into the attP2 landing site are homozygous viable. Of the 7,623 lines generated by R. Ueda *et al.* by P-element transformation, 54% are associated with lethality or semilethality when homozygous (numbers extracted from the information available at <http://www.shigen.nig.ac.jp/fly/nigfly/>). Similarly, among the 22,270 lines established by G. Dietzl *et al.* by the same mechanism, 5.4% were associated with sterility and 17.5% with lethality when homozygous (numbers extracted from Supplementary Table 2 of ref. 1). The inability to create homozygotes of P-element-integrated UAS-hairpin lines is a potential drawback to the



transgenic hairpin technology, given that a twofold increase in gene expression can have a strong effect on phenotype (as discussed below). Finally, the high rate of false negatives, resulting from random integration into poorly expressed loci, is automatically eliminated by inserting RNAi constructs into an optimal site such as attP2.

To ask how temperature, the amount of Gal4 and the number of UASs affect the severity of hairpin-induced phenotypes, we carried out a number of tests using a sensitive wing assay whereby an RNAi construct against *Notch* is expressed under the control of the enhancer trap C96-Gal4 driver⁶. C96-Gal4 is expressed in the region of the wing imaginal disc that gives rise to the dorsal-ventral margin⁷, and a reduction of Notch activity at the margin generates dose-dependent phenotypes ranging from mild loss of margin bristles to strong wing notching (Fig. 2a). We generated two independent hairpins against *Notch* and examined their phenotypes when driven by C96-Gal4 at both 25 °C and 29 °C. As expected from our previous results, both *Notch* hairpin constructs behaved similarly (Supplementary Fig. 1 online). However, we observed marked differences in the expressivity of the phenotypes between males and females, as has been seen with other hairpin constructs (as discussed above). Further, the severity of the phenotypes was dependent on temperature, most likely reflecting the temperature sensitivity of the Gal4-UAS system⁸. Control hairpins did not produce any phenotype of note.

Next, we compared the effect of 5×, 10× and 20× UAS-*Notch hp2* in the presence of one copy of C96-Gal4. The 5× UAS line was generated as a derivative of the 10XUAS-*Notch hp2* line after excision of the Cre-loxP cassette (Supplementary Methods). A recombinant chromosome was generated between C96-Gal4 and 10XUAS-*Notch hp2* to produce the various genotypes shown in Figure 2b. Analyses of the various combinations revealed a continuous phenotypic series from the 5× to the 20× UAS hairpin dose, demonstrating that expressivity can be manipulated by



altering the number of UAS sites in addition to the hairpin copy number. To examine the effect of varying the amount of Gal4, we compared the effects of one copy versus two copies of C96-Gal4 in the presence of one copy and two copies of 10XUAS-Notch hp2. In all situations in which the dose of C96-Gal4 was increased, a significant enhancement of the phenotype was observed, as we detected a large fraction of flies with the most extreme (Class 5) wing-notching phenotypes. Notably, little enhancement was observed between one copy and two copies of 10XUAS-Notch hp2 when two copies of C96-Gal4 were present. Further, doubling the amount of Gal4 had a more profound effect than doubling the number of UAS hairpins, indicating that the amount of Gal4 in these experiments is more limiting. This is consistent with the relatively weaker phenotype observed in C96-Gal4, 10XUAS-Notch hp2/10X-UASGFP compared to C96-Gal4, 10XUAS-Notch hp2/+, where presumably the amount of Gal4 available for activation of the 10× UAS is titrated by the 10× UASGFP (Fig. 2b). Note, however, that the effect is only clearly detected at 25 °C, which is consistent with the temperature sensitivity of the Gal4-UAS system.

In conclusion, in our experiments with C96-Gal4, the amount of Gal4 was more critical than the number of UASs for generating strong hairpin-induced phenotypes. It is important to note that because the C96-Gal4 line is a relatively weak driver (data

Figure 2 | Parameters of *in vivo* RNAi using Valium. (a) Five classes of wing phenotypes were distinguished when a Notch hairpin was expressed using the wing margin C96-Gal4 driver. Class 1, wild type or a few bristles missing; class 2, margin bristles missing but no notches; class 3, moderate wing notching; class 4, extensive wing notching; class 5, most of the wing margin missing. (b) Phenotypes of C96-Gal4, Notch-hp2 flies. The phenotypes are stronger at 29 °C than at 25 °C and in males than in females; the two hairpins have similar expressivity. The effect of varying the number of UASs, the amounts of Gal4 and Dcr2 are shown using UAS-Notch hp2. More than 50 wings were scored in each experiment. Details of the construction of the various genotypes can be found in the **Supplementary Note** online.

not shown), we expect that, in conditions where the driver is stronger, the number of UASs may be the most important parameter to optimize in order to improve the severity of hairpin-based phenotypes.

Recently, Dietzl *et al.* reported that increasing the level of Dicer 2 (Dcr 2) increases the potency of the RNAi hairpin phenotype, most likely by increasing the processing of long dsRNAs¹. Thus, we compared the phenotype of C96-Gal4, 10XUAS-Notch hp2/+ and UAS-Dcr2/+; C96-Gal4, 10XUAS-Notch hp2/+ flies. Consistent with these findings, overexpressing Dcr2 along with the hairpin construct increased the severity of the phenotype, but not as much as doubling the amount of Gal4 (Fig. 2b).

Note: Supplementary information is available on the Nature Methods website.

ACKNOWLEDGMENTS

We thank G. Rubin, C. Zuker, K. Moses and B. Mathey-Prevot for critical input on the project, B. Dickson (IMP, Vienna) for the gift of UAS-Dcr2 and F. Karch (University of Geneva) for nanos-integrase. M.M. is a fellow of the Jane Coffin Childs Memorial Fund. M.B. is supported by R01 GM067761 from the US National Institute of General Medical Sciences. This work was supported in part by the Janelia Farm Visitor program. N.P. is an investigator of the Howard Hughes Medical Institute.

Published online at <http://www.nature.com/naturemethods/>
Reprints and permissions information is available online at
<http://npg.nature.com/reprintsandpermissions>

- Dietzl, G. *et al.* *Nature* **448**, 151–156 (2007).
- Brand, A.H. & Perrimon, N. *Development* **118**, 401–415 (1993).
- Groth, A.C., Fish, M., Nusse, R. & Calos, M.P. *Genetics* **166**, 1775–1782 (2004).
- Perrimon, N. & Mathey-Prevot, B. *Genetics* **175**, 7–16 (2007).
- Bischof, J., Maeda, R.K., Hediger, M., Karch, F. & Basler, K. *Proc. Natl. Acad. Sci. USA* **104**, 3312–3317 (2007).
- Presente, A., Shaw, S., Nye, J.S. & Andres, A.J. *Genesis* **34**, 165–169 (2002).
- Gustafson, K. & Boulianne, G.L. *Genome* **39**, 174–182 (1996).
- Mondal, K. *et al.* *J. Mol. Biol.* **370**, 939–950 (2007).
- Fridell, Y.W. & Searles, L.L. *Nucleic Acids Res.* **19**, 5082 (1991).
- Siegal, M.L. & Hartl, D.L. *Genetics* **144**, 715–726 (1996).
- An, X., Armstrong, J.D., Kaiser, K. & O'Dell, K.M. *J. Neurogenet.* **14**, 227–243 (2000).

Vector and parameters for targeted transgenic RNA interference in *Drosophila melanogaster*

Jian-Quan Ni, Michele Markstein, Richard Binari, Barret Pfeiffer, Lu-Ping Liu, Christians Villalta, Matthew Booker, Lizabeth Perkins & Norbert Perrimon

Supplementary text and figures:

Supplementary Table 1 Positive gene set used to test the efficacy of Valium.

Supplementary Methods

Supplementary Figure 1 Two different Notch hairpin constructs behave similarly.

Supplementary Note

SI Table 1: Positive gene set used to test the efficacy of Valium. Information on the hairpin lines generated against Epidermal Growth Factor Receptor (EGFR), Son of sevenless (Sos); sprouty (sty), decapentaplegic (dpp), cubitus interruptus (ci), armadillo (arm), domeless (dome), hopscotch (hop), Stat92, disc-large (dlg), and RacGap50C (RacGap). Two independent constructs were generated for most genes.

TABLE 1

Line Gal4 at 29°C	CG#/gene	Oligos	Size of fragment	Phenotype with en-
TR00039A.1	CG10079/EGFR	F: 5'-GTCTAGACTATGCAAGTTGCGCATTGT-3'; R: 5'-AGAATTCGGAGTCTGCACCAGGACATT -3'	443bp	growth and vein defects
TR00040A.1	CG10079/EGFR	F: 5'-GTCTAGAACAAGAGCAGGGATCGCTAA -3'; R: 5'-AGAATTCGGCAGTTATCTTGCTGCTCC-3'	424bp	growth and vein defects
TR00380A.1	CG7793/Sos	F: 5'-GTCTAGAGAAAACGAATCTGGAGCGAG-3'; R: 5'- AGAATTC AACACGATATTGTACCCGC-3'	413bp	growth and vein defects
TR00606A.1	CG7793/Sos	F: 5'- GTCTAGACTGGATCTGGA ACTCTCGCT-3'; R: 5'- AGAATTCTACTGGCAGTGCTATGCGTT-3'	435bp	growth and vein defects
TR00024A.1	CG1921/sty	F: 5'-GTCTAGAGTCTGAACCAGCCCATCATC-3'; R: 5'-AGAATTCATGGGCCAGTAGAACCCACAG-3'	463bp	vein defects
TR00025A.1	CG1921/sty	F: 5'-GTCTAGAGCAGCTGTCTGAATCTGCAA-3'; R: 5'-AGAATTC AAGGTCAGGTGGTGGATCTG-3'	480bp	vein defects
TR00047A.1	CG9885/dpp	F: 5'-GTCTAGACCAGCACAGCATTAGCAAAA -3'; R: 5'-AGAATTCCTCCTTGCTGTAGGTGGA-3'	441bp	veins missing
TR00048A.1	CG9885/dpp	F: 5'-GTCTAGAAACAATATGAATCCCGCAA -3'; R: 5'-AGAATTCGGACTCTGCGCTCTCAAATC-3'	470bp	veins missing
TR00709A.1	CG2125/ci	F: 5'-GTCTAGAGAGCTCTTTGGGTGAACTGC-3'; R: 5'-AGAATTCGTGTGGTGTGCATCGGATT-3'	402bp	crossvein missing
TR00710A.1	CG2125/ci	F: 5'-GTCTAGAAGCAGCCTTCATCGACATCT-3'; R: 5'-AGAATTCGTGTGGCTTTTCACCGGTAT-3'	446bp	crossvein missing
TR00681A.1	CG11579/arm	F: 5'-GTCTAGAGAAAGTGCTCTCCGTTTGCT -3'; R: 5'-AGAATTC CGTGATGGTGGATGCAATAG-3'	544bp	margin defects
TR00706A.1	CG14226/dome	F: 5'-GTCTAGACATCACTTCACCACGTCACC -3'; R: 5'-AGAATTCCTTACGCGGAATGTATCGGT-3'	566bp	extra vein
TR00703A.1	CG1594/hop	F: 5'-GTCTAGAAAAGTTGGCGCTTGCTAAAA -3'; R: 5'-AGAATTCGTTGAACACACGGATTGTGC-3'	507bp	extra vein
TR00704A.1	CG1594/hop	F: 5'-GTCTAGACGACGATGGCATGATGTTA -3'; R: 5'- ACAATTGATAGCCGGGATCGCTAATTT-3'	442bp	extra vein
TR00701A.1	CG4257/Stat92	F: 5'-GTCTAGAAAGCTGCTTGCCCAAAACTA -3'; R: 5'-AGAATTCGTCGACGATAAAGGCAGAGC-3'	402bp	extra vein
TR00702A.1	CG4257/Stat92	F: 5'-GTCTAGATACGCGCAATACACAGATGG -3'; R: 5'-AGAATTCATCAATGGTCAGAGAACGCC-3'	442bp	extra vein
TR00031A.1	CG1730/dlg	F: 5'-GTCTAGAGAATGGCGATGATAGCTGGT -3'; R: 5'-AGAATTCATTGAGAAGCCCAGTCCCTT-3'	414bp	crumbled wings
TR00051A.1	CG13345/RacGap	F: 5'-GTCTAGATTGGCCTCTATCGATTGTCC -3'; R: 5'-AGAATTCCTGGGTGAAAACCTCCGTGT-3'	428bp	vein defects, crumbled wings

S2. Materials and Methods

Construction of Valium. The SV40 polyadenylation signal sequence of the *Drosophila* transformation vector pUAST (Brand and Perrimon, 1993) was amplified using the specific primers SV40-SacII (5'-GCCGCGGGATCTTTGTGAAGGAACCTTAC-3') and SV40-SacI (5'-GGAGCTCTGGAACCAGACATGATAAGATAC-3'), sequenced and subcloned into pBluescript (Stratagene). The *ftz* intron (Read and Manley, 1992; Rio, 1988) was amplified using genomic DNA as the template and the specific primers ftz-XbaI-MfeI (5'-CTCTAGACAATTGTTGGCATCAGGTAGGCATCA-3') and ftz-SacII (5'-ACCGCGGCTCTAGTTCTTTGCAATCTGTA-3'). After sequencing, the correct fragment was subcloned into SV40-pBluescript. Loxp1 and Loxp2 oligonucleotides (Loxp1-HindIII: 5'-AGCTTATAACTTCGTATAATGTATGCTATACGAAGTTATCTGCA-3'; Loxp1-PstI: 5'-GATAACTTCGTATAGCATAACATTATACGAAGTTATA-3') (Loxp2-NcoI: 5'-GACCATGGATAACTTCGTATAATGTATGCTATACGAAGTTATG-3'; Loxp2-BamHI: 5'-GATCCATAACTTCGTATAGCATAACATTATACGAAGTTATCCATGGTCTGCA-3') were denatured at 95°C and after annealing were subcloned into ftz-SV40-pBluescript. One 5XUAS cassette of pUAST was amplified by the specific primers (UAS-PstI (5'-TCTGCAGGCAGGTCGGAGTACTGTCC-3'); UAS-NcoI (5'-TCCATGGCTCCGCTCGGAGGACAGTA-3'), and another 5XUAS cassette was amplified by primers UAS-BamHI (5'-TGGATCCGCAGGTCGGAGTACTGTCC-3') and UAS-SalI (5'-AGTCGACCTCGCTCGGAGGACAGTA-3'). Both were confirmed by sequencing and then subcloned individually into Loxp1-Loxp2-ftz-SV40-pBluescript. The HSP70 promoter was amplified from pUAST using the specific primers HSP70-SalI (5'-GGTCGACAGCGAGCGCCGAGTATAAAT-3') and HSP70-EcoRI-BglII-XbaI (5'-GTCTAGAGCAGATCTGCGAATTCCCAATTCCCTATTC-3'). The correct PCR product was subcloned into Loxp1-5XUAS-Loxp2-5XUAS-ftz-SV40-pBluescript. Two DNA fragments, one containing the Hind III, EcoRV, ClaI, XhoI and KpnI restriction sites, and another containing the EcoRI, NotI, SpeI, NheI, XbaI, NdeI, BglII and MfeI sites were cloned into Loxp1-5XUAS-Loxp2-5XUAS-HSP70-ftz-SV40-pBluescript. The attB fragment in pCa4 (Microbix Biosystems) was amplified using attB-Xho (5'-CTCGAGGCTGCATCCAACGCGTTGG-3') and attB-KpnI (5'-GGTACCGAATTAGGCCTTCTAGTGGAT-3'). Subsequently, the correct PCR product was introduced into Loxp1-5XUAS-Loxp2-5XUAS-HSP70-ftz-SV40-pBluescript. The 1.8kb DNA fragment which contains both the regulatory and coding regions of *vermillion* was cut by HindIII from pYC1.8 (kindly provided by Lillie Searles), and then subcloned into AttB-Loxp1-5XUAS-Loxp2-5XUAS-HSP70-ftz-SV40-pBluescript. A small *white* intron from pWIZ (Lee and Carthew, 2003) was cut by NheI/SpeI and then subcloned into the restriction sites of AttB-Loxp1-5XUAS-Loxp2-5XUAS-HSP70-ftz-SV40-pBluescript. Finally, the EcoRI/MfeI restriction sites in *vermillion* and the SV40 polyadenylation tail were destroyed by specific mutations using the QuickChange site-directed mutagenesis kit (Stratagene). The mutant plasmid was generated with two pairs of mutagenesis primers (EcoRI-F: 5'-CTCCGAGTTGCGAATCGAGTTCCGCGCCTCCTCGTC-3'; EcoRI-R: 5'-GACGAGGAGGCGCGGAACCTCGATTCGCAACTCGGAG-3'; MfeI-F1: 5'-GCATAGCCAAACATTGACGAATTGGATACCCTGCCGATTG-3'; MfeI1-R: 5'-CAATCGGCAGGGTATCCAATTTCGTCATGTTTGGCTATGC-3').

Generation of 5XUAS hairpin derivative. The pentamer of UAS was flanked by two minimal *loxP* sites which each contain an 8bp asymmetric core sequence and two 13bp inverted repeats. By crossing a 10XUAS line with a line containing the Cre enzyme (Oberstein et al., 2005), one pentamer of UAS can be easily removed. Specifically, virgin females of genotype *y w, P[y+Cre]1b; D/TM3, Sb* were crossed to males of genotype *y v/Y; 10XUAS hairpin/10X-UAS hairpin*. In the F1 generation, males of genotype *y w, P[Cre]1B/Y; 10XUAS-hairpin/TM3, Sb* were isolated and crossed en masse to virgin females of genotype *y v; Sb/TM3, Ser*. Among the resulting progeny, males of genotype *y v/Y; putative 5XUAS-hairpin/TM3, Ser* were isolated and mated individually to virgin females of genotype *y v; Sb/TM3, Ser*. Sib progeny of genotype *y v; putative 5XUAS hairpin/TM3, Ser* from this cross were mated inter se to establish homozygous stocks of genotype *y v; 5XUAS hairpin/5XUAS hairpin*. To verify the loss of one of the 5XUAS cassettes from individual lines, genomic DNA from single males was amplified by PCR using primers UAS-F (5'-AGAAGGCCTAATTCGGTACC-3') and UAS-R (5'-GCGCCTCTATTTATACTCCG-3'). Using these primers, the presence of both 5XUAS cassettes will generate a band of ~400bp, while the presence of only one of the cassettes will generate a band of ~200bp.

Hairpin design and construction. Primers for hairpins were designed using the DRSC amplicon design tool that we refer to as SnapDragon (http://www.flyrnai.org/cgi-bin/RNAi_find_primers.pl <http://www.flyrnai.org/cgi-bin/RNAi_find_primers.pl>). To construct the hairpins, we first identified regions of 400-600bp that are free of EcoRI (or MfeI) and XbaI (or SpeI, AvrII) and that are free of 19bp predicted off targets. If this was not possible, then regions with either no 20 or 21bp matches to other genes were used. Blast analyses were performed on genomic and cDNA sequences. In most cases the hairpin sequences were selected to be within a single exon. However, when this was not possible, we used post-spliced transcript sequence for the design and ensured that splice sites AG/GTRAGT, TTTYYYTNCAG/RT (R for A or G; Y for C or T; and N for any base) were not present. We then added XbaI (or SpeI, AvrII) cutting sites to the 5' end of the forward primer and EcoRI (or MfeI) to the 5' end of the reverse primer. PCR products were cut by EcoRI (or MfeI) and XbaI (or SpeI, AvrII). Following gel purification, the DNA fragment was sequentially subcloned twice into XbaI, MfeI, EcoRI and SpeI sites of Valium. Since digests with either EcoRI and MfeI, or SpeI, AvrII and XbaI result in compatible cohesive ends, a single PCR product can be cloned in both orientations in the Valium multiple cloning site (MCS) that contains EcoRI, SpeI, AvrII, XbaI and MfeI restriction sites.

Establishment of transgenic RNAi hairpin lines. Lines were established either in our lab or at Genetic Services, Inc (GSI, <http://www.geneticservices.com>). In the Perrimon lab, construct DNA and capped integrase mRNA were co-injected into embryos of genotype *y v; attP2/attP2*. We used the attP2 site since it has been shown to be optimal for the induction of UAS-constructs with several Gal4 drivers (Markstein et al., submitted). The capped integrase mRNA was prepared as previously described (Groth et al., 2004). Briefly, the pET11-C31-polyA plasmid was cut by BamHI, digested by proteinase K, then extracted with phenol-chloroform, precipitated, and finally resuspended in RNase-

free water. 1 ug of linear DNA was used to transcribe the integrase RNA using the mMESSAGE mMACHINE T7 transcription system (Ambion). The resulting mRNA was resuspended in RNAase-free injection buffer and then mixed with the hairpin-construct before injection. Surviving Go individuals were individually crossed to *y v; Sb/TM3, Ser* and *y+ v+* progeny from these crosses were individually back-crossed to *y v; Sb/TM3, Ser* to establish homozygous stocks. About 25% transformants were usually recovered using this approach.

At GSI, construct DNA was injected into a *y w, nanos integrase; attP2/attP2* stock. Surviving Go males were then individually crossed to *y v; attP2/attP2* virgin females, and *y+v+* males in the progeny were selected and individually back-crossed to *y v; Sb/TM3, Ser* virgin females to establish homozygous stocks.

Due to the presence of background lethal(s) on some of the attP2 chromosomes about 5% of the transformed lines cannot be homozygosed. These lines were discarded and the DNA reinjected. Once homozygous lines were established, flies were checked by PCR for the presence of the hairpin constructs. The presence of the two inverted DNA repeats in transgenic flies was confirmed by two PCR reactions using the following oligos: HSP-forward: 5'-CGCAGCTGAACAAGCTAAAC -3'; *gene X*-forward; and *ftz*-reverse: 5'-TAATCGTGTGTGATGCCTACC -3'.

Notch hairpins. We used two different hairpin constructs in this study. For *Notch hairpin 1*, a 402bp fragment was amplified using: F: 5'-GTCTAGAATTGTCCCAGTGGCTTTACG-3'; R: 5'-AGAATTCCGCAATTCTGACCCTGAAAT-3'. For *Notch hairpin 2*, a 406bp fragment was amplified with F: 5'-GTCTAGAATCGGATCTATTGGCACAGG-3'; R: 5'-AGAATTCGTTCCACCGCTTCGGTATTGT-3'.

Stocks. The following stocks were used: *w; C96-Gal4* (homozygous viable on the 3rd chromosome (Gustafson and Boulianne, 1996)); *w; en-Gal4 UAS-GFP* (homozygous viable on the 2nd chromosome, from our lab); *y w nanos-Integrase phiC31* was obtained from F. Karch (Bischof et al., 2007) and *w; UAS-Dcr2* (homozygous on the 2nd) from B. Dickson (Dietzl et al., 2007).

Wing preparation and scoring. Flies were dehydrated in 100% EtOH overnight and then mounted in Hoyer's medium with lactic acid and photographed with a Zeiss Axiophot. At least 50 individual wings were scored in each experiment.

References:

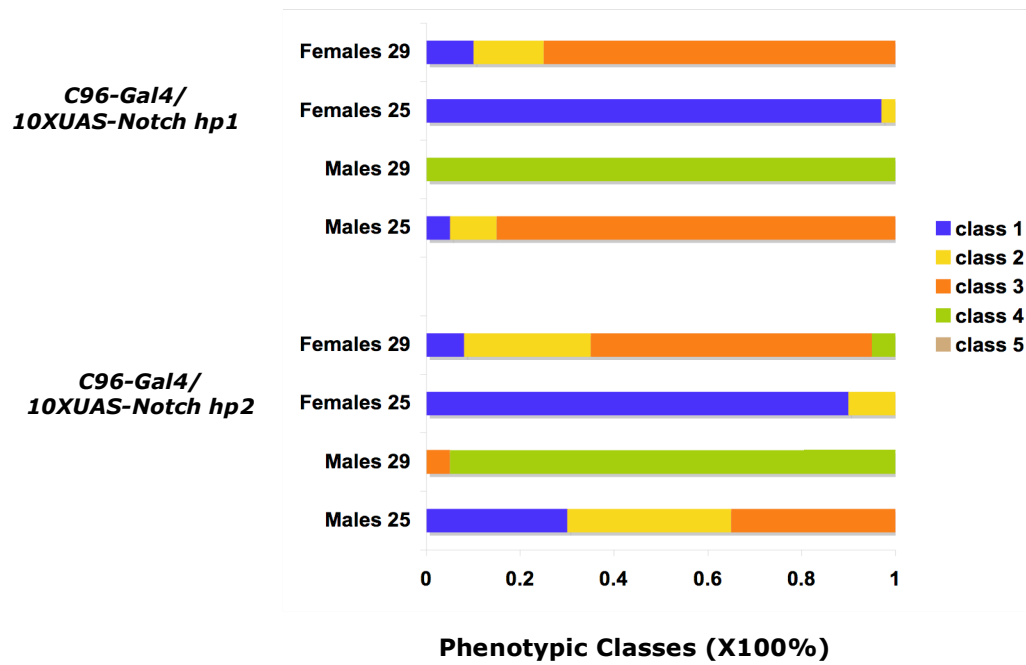
- Bischof, J., Maeda, R.K., Hediger, M., Karch, F. & Basler, K. An optimized transgenesis system for *Drosophila* using germ-line-specific phiC31 integrases. *Proc Natl Acad Sci U S A* **104**, 3312-7 (2007).
- Brand, A.H. & Perrimon, N. Targeted gene expression as a means of altering cell fates and generating dominant phenotypes. *Development* **118**, 401-15 (1993).
- Dietzl, G. et al. A genome-wide transgenic RNAi library for conditional gene inactivation in *Drosophila*. *Nature* **448**, 151-6 (2007).
- Groth, A.C., Fish, M., Nusse, R. & Calos, M.P. Construction of transgenic *Drosophila* by

- using the site-specific integrase from phage phiC31. *Genetics* **166**, 1775-82 (2004).
- Gustafson, K. & Boulianne, G.L. Distinct expression patterns detected within individual tissues by the GAL4 enhancer trap technique. *Genome* **39**, 174-82 (1996).
- Lee, Y.S. & Carthew, R.W. Making a better RNAi vector for *Drosophila*: use of intron spacers. *Methods* **30**, 322-9 (2003).
- Oberstein, A., Pare, A., Kaplan, L. & Small, S. Site-specific transgenesis by Cre-mediated recombination in *Drosophila*. *Nat Methods* **2**, 583-5 (2005).
- Read, D. & Manley, J.L. Alternatively spliced transcripts of the *Drosophila* tramtrack gene encode zinc finger proteins with distinct DNA binding specificities. *Embo J* **11**, 1035-44 (1992).
- Rio, D.C. Accurate and efficient pre-mRNA splicing in *Drosophila* cell-free extracts. *Proc Natl Acad Sci U S A* **85**, 2904-8 (1988).

S3. Supplementary Figure 1:

Two different *Notch* hairpin constructs behave similarly. The wing phenotypes *C96-Gal4/+; 10XUAS-Notch-hp1/+* and *C96-Gal4/+; 10XUAS-Notch-hp2/+* were scored at different temperatures.

Supplementary FIGURE 1



Supplementary Note

The various genotypes are:

- *C96-Gal4*, *5XUAS-Notch hp2*: *C96-Gal4/+*; *5XUAS-Notch-hp2/+*
- *C96-Gal4*, *10XUAS-Notch hp2*: *C96-Gal4/+*; *10XUAS-Notch-hp2/+*
- *C96-Gal4*, (*10XUAS-Notch hp2*)^{X2}: *C96-Gal4/+*; *10XUAS-Notch-hp2/10XUAS-Notch-hp2*
- (*C96-Gal4*)^{X2}, *10XUAS-Notch hp2*: *C96-Gal4/ C96-Gal4*, *10XUAS-Notch hp2/+*
- (*C96-Gal4*)^{X2}, (*10XUAS-Notch hp2*)^{X2}: *C96-Gal4/ C96-Gal4*, *10XUAS-Notch hp2/10XUAS-Notch hp2*
- *C96-Gal4*, *10XUAS-Notch hp2*, *10XUAS-GFP*: *C96-Gal4/+*; *10XUAS-Notch-hp2/10XUAS-GFP*
- *C96-Gal4*, *UAS-Dcr2*, *10XUAS-Notch hp2*: *C96-Gal4/UAS-GFP*; *10XUAS-Notch-hp2/+*